Capillary Flow Layer-by-Layer: A Microfluidic Platform for the High-Throughput Assembly and Screening of Nanolayered Film Libraries

Steven A. Castleberry,[†,‡,§,⊥] Wei Li,[†,‡,⊥,#] Di Deng,[∥] Sarah Mayner,[†] and Paula T. Hammond[†,‡,*]

[†]Department of Chemical Engineering, Massachusetts Institute of Technology, Cambridge, Massachusetts, United States, [‡]Koch Institute of Integrative Cancer Research, Massachusetts Institute of Technology, Cambridge, Massachusetts, United States, [§]Harvard-MIT Division of Health Sciences and Technology, Cambridge, Massachusetts, United States, and [∥]Department of Materials Science and Engineering, Massachusetts Institute of Technology, Cambridge, Massachusetts, United States. [⊥]S. Castleberry and W. Li contributed equally to this work. [#]Present address: Department of Chemical Engineering, Texas Tech University, Lubbock, TX, United States.

ABSTRACT Layer-by-layer (LbL) assembly is a powerful tool with increasing real world applications in energy, biomaterials, active surfaces, and membranes; however, the current state of the art requires individual sample construction using large quantities of material. Here we describe a technique using capillary flow within a microfluidic device to drive high-throughput assembly of LbL film libraries. This capillary flow layer-by-layer (CF-LbL) method significantly reduces material waste, improves quality control, and expands the potential applications of LbL into new research spaces. The method can be operated as a simple lab benchtop apparatus or combined with liquid-handling robotics to extend the library size. Here we describe and demonstrate the technique and establish its ability to recreate and expand on the known literature for film growth and morphology. We use the same platform to assay biological properties such as cell adhesion and proliferation and ultimately provide an example of the use of this approach to identify LbL films for surface-based DNA transfection of commonly used cell types.

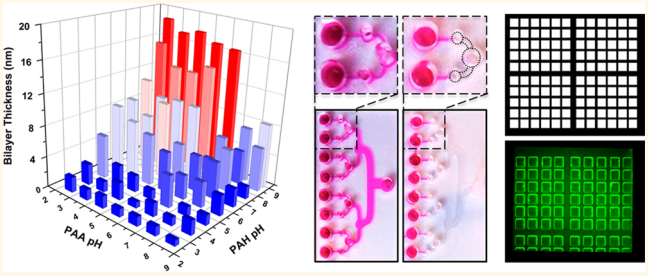

KEYWORDS: layer-by-layer · LbL · high-throughput · polyelectrolyte multilayers · PEM · screening · ultrathin films

Layer-by-layer (LbL) assembly is the alternating adsorption of materials onto a surface using complementary interactions, one layer of material at a time, creating nanometer-scale thin films.[1−4] This process enables fine control over the assembly of functional materials into ultrathin coatings that exhibit a range of interesting properties and have found diverse applications in reactive membranes, drug delivery systems, and electrochemical and sensing devices.[5−8] Over the past decade, exciting new developments have demonstrated the power of LbL assembly in biomedical applications, with examples ranging from bone tissue engineering[9,10] to vaccine delivery[11] and creating biological interfaces.[12,13]

Several recent advances have led to the adaptation of LbL toward commercial translation, including the use of convection in automated spray-LbL[14,15] to coat a broad range of surfaces with accelerated cycle times and the use of spin-assisted LbL[16−18] to generate thin films on planar surfaces with control of molecular orientation. Researchers have also explored using microfluidics to coat channels[19] and microparticles[20] *via* alternating flow of polyelectrolytes. These contributions are important, as they demonstrate the generalizability of the LbL process and provide insight into the assembly of uniform films of a given composition. These advances enable the implementation of promising LbL systems at the speed and throughput needed for commercial products and processes; however, to date there is no approach capable of assembling libraries of LbL films for research, development, and optimization.

Attempts to create and examine libraries of different LbL film systems can yield understanding of the impact of simple compositional changes in the polymers

* Address correspondence to hammond@mit.edu.

Received for review April 8, 2014 and accepted May 16, 2014.

Published online May 16, 2014
10.1021/nn501963q

incorporated on final film structure and property.[21−23] The existing methods for LbL assembly for new materials discovery, however, rely on the individual production of film samples using large reservoirs of material and must generally be facilitated using specialized or modified lab equipment.[24−26] The limitations of current LbL techniques are particularly significant when precious, rare, and costly materials are incorporated in the film assembly. For biomaterials applications in particular, optimizing incorporation and/or release of siRNA, DNA, active growth factors, engineered peptides, or other therapeutics would require significant quantities of material, thus severely limiting investigations and potential discoveries in these areas.

As research into LbL film technology continues to expand and researchers pursue new discoveries along with commercial translation in the pharmaceutical industry, several challenges need to be overcome. These include simplifying *in vitro* analysis of films, improving material conservation, and making the LbL process more accessible to a broader scientific community. To address these challenges and enable more thorough investigations of LbL film assemblies, we have developed a simple microfluidic approach for the high-throughput construction of multiple LbL films in parallel. We have termed this approach "capillary flow layer-by-layer" (CF-LbL), as we harness capillary action to fill microchannels in which LbL films are assembled. The CF-LbL device consists of an array of these microchannels formed by bonding a polydimethylsiloxane (PDMS) mold to an oxygen plasma treated substrate (glass, silicon, *etc.*). This approach requires as little as 0.1% as much material per film compared to conventional methods, while enabling the simultaneous assembly of nearly 400 times as many independent films. LbL assemblies of varying compositions, morphologies, and architectures can be rapidly produced in a format that suits a number of physicochemical and *in vitro* biological assays and screened for meaningful material properties using this method.

RESULTS AND DISCUSSION

Each microchannel is composed of a main channel where material from solution adsorbs onto the substrate, as well as three openings: an inlet well (1), a capillary flow break well (2), and an exit well (3) (Figure 1a). Capillary flow within the channel is controlled by covering select regions of the PDMS mold during plasma treatment (Figure 1c and Supplementary Figure 1). This leaves these regions hydrophobic, while the uncovered areas receive plasma treatment and become hydrophilic. Material held within the channel is cleared by vacuum, which is selectively applied by covering both holes 2 and 3 simultaneously (Figure 1b). The layout of channels is modular by design and can be based on 96- and 384-well plate dimensions for high-throughput screening or consists of only a few microchannels

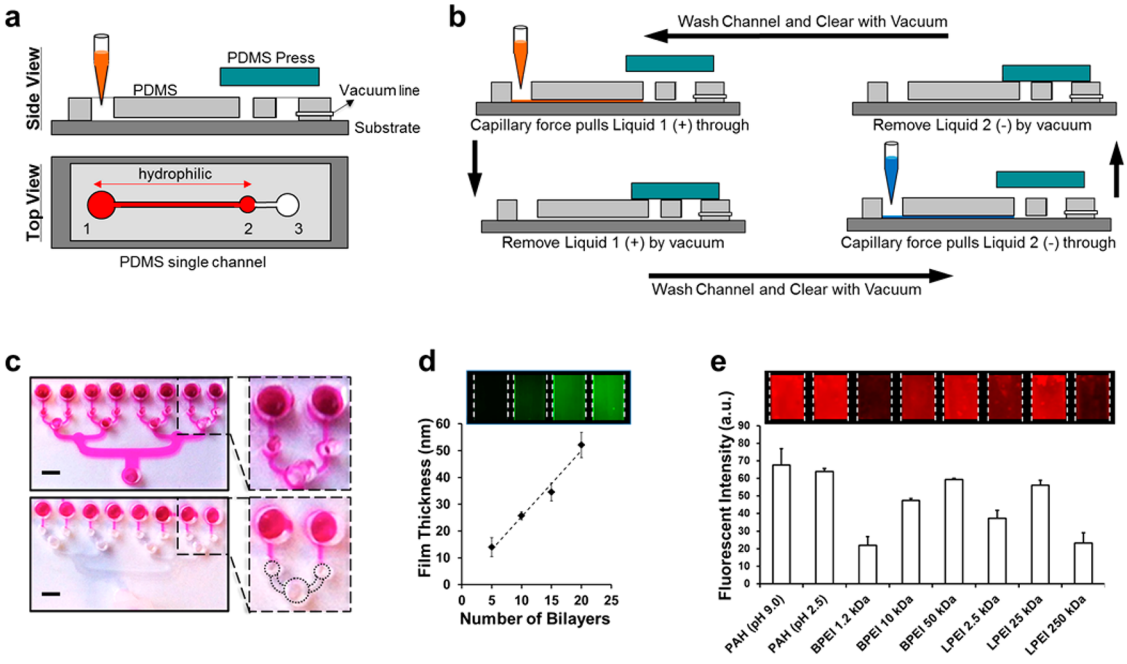

Figure 1. Design of capillary flow layer-by-layer (CF-LbL) device. (a) Top and side view of a single channel within a CF-LbL device; the red region is O_2 plasma treated. (b) The process of alternating adsorption of material inside the microfluidic channels, (+) polycation and (−) polyanion species. (c) Multiple independent channels within a single CF-LbL device. The top image is fully O_2 plasma treated; the bottom image selectively treated; scale = 3 mm. (d) Measurement of film thickness for a sample PAA/PAH_{FITC} LbL film. (e) Screening LbL film architectures for material incorporation. Fluorescently labeled PAA is incorporated into bilayer LbL films with the polycations PAH, branched polyethylenimine (BPEI), and linear polyethylenimine (LPEI). Data shown as mean ± SD. Channels used were 800 μm wide and 2.0 mm long.

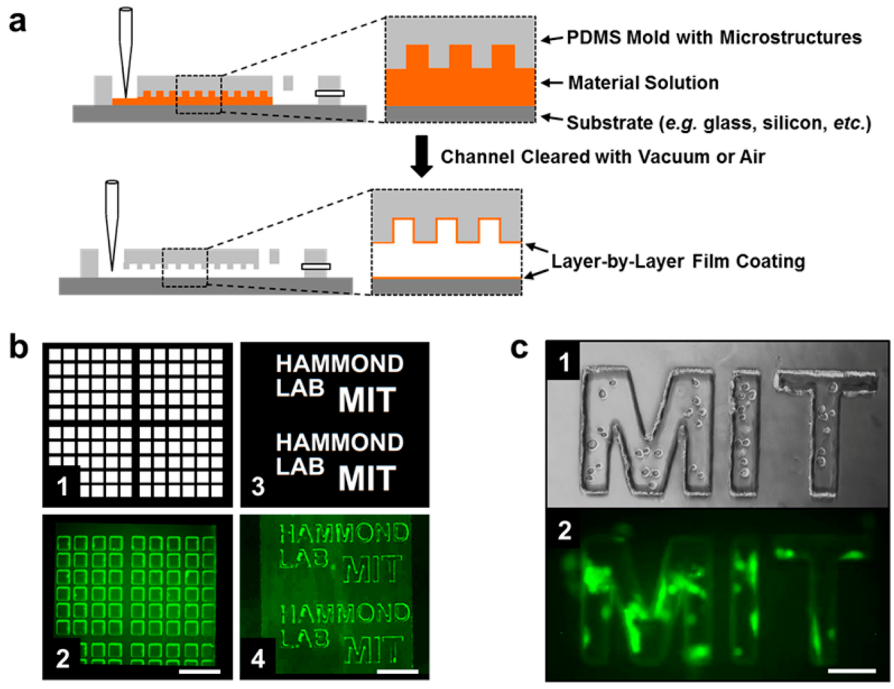

Figure 2. CF-LbL coating of microstructures contained within microchannels for diverse customized applications. (a) Schematic for the coating of microstructures within the CF-LbL channels. (b) Demonstration of patterned microstructures included within the microchannels; (1 and 3) lithographic mask designs for the microwells; (2 and 4) fluorescent imaging of channels containing microstructures coated with PAA/PAH_{FITC}. Scale bar = 150 μm. (c) Micropatterned surface within the channel used to direct NIH-3T3 cell seeding. (1) Imaged immediately after clearing uncaptured cells from main channel with media. (2) Fluorescent imaging of spread cells after 24 h. Scale bar = 50 μm. Channels used were 800 μm wide and 1.2 mm long. Channels shown are 500 μm wide and 5.0 mm long.

for easy benchtop use (Supplementary Figure 2). The characterization of films assembled within the microchannels is performed similarly to those created by existing LbL methods using ellipsometry, profilometry, light microscopy, and atomic force microscopy.

To demonstrate the application of this technology in the construction and evaluation of LbL films, we began by assembling a simple bilayer film architecture of poly(acrylic acid) (PAA) and poly(allylamine hydrochloride) (PAH). PAH was labeled with a fluorescent dye, and the growth of the film was measured by profilometry. The film grew linearly and resembles similar films assembled on glass slides constructed *via* dip LbL technique (Figure 1d) with regard to thickness per bilayer. For current LbL assembly techniques, investigating libraries of LbL films is a very time- and material-intensive task, as it requires up to multiple days to construct a single sample while using milliliters of material solution.[27−29] To demonstrate this capability with CF-LbL, we assessed the incorporation of a labeled polyanion (PAA) with candidate polycations in simple bilayer assemblies (Figure 1e). This experiment demonstrates that by using common lab imaging modalities, such as a gel imager, arrays of LbL films can be assessed for material incorporation. This type of approach could be very useful in determining the best polymer pairing for incorporation of a material of interest, such as a small molecule drug or protein therapeutic.

The layout and design of the microchannels within the device are easily customized for different applications. Channel parameters such as length, width, and shape can be modified by designing different lithographic masks for creating the PDMS mold; however, using more recent advances in soft lithography techniques we can incorporate even more diverse designs. This includes the capability to incorporate microstructures as a part of the PDMS mold that forms the channel, which can be accomplished *via* multilayer soft lithography.[30] Introducing microstructures within the channel opens many interesting avenues for investigation, particularly in the area of *in vitro* experiments, where the structures could be used to influence cell behavior.

Microstructures contained within the channels of the device can be uniformly coated with LbL films, similar to coating flat surfaces (Figure 2a). These structures can be used to increase the active surface area within the channel and influence cell-surface interactions and adhesion, allowing for the generation of patterned cell surfaces. To demonstrate the capability of CF-LbL to coat these microstructures, we assembled a simple bilayer film of PAA/PAH using a fluorescently labeled PAH. Fluorescent imaging of the coated channels shows the uniformity of the film coating, with well-reproduced films assembling within and around the microstructure features (Figure 2b).

The use of microstructures, such as microwells, in cell sampling and small-scale cell culture has been well

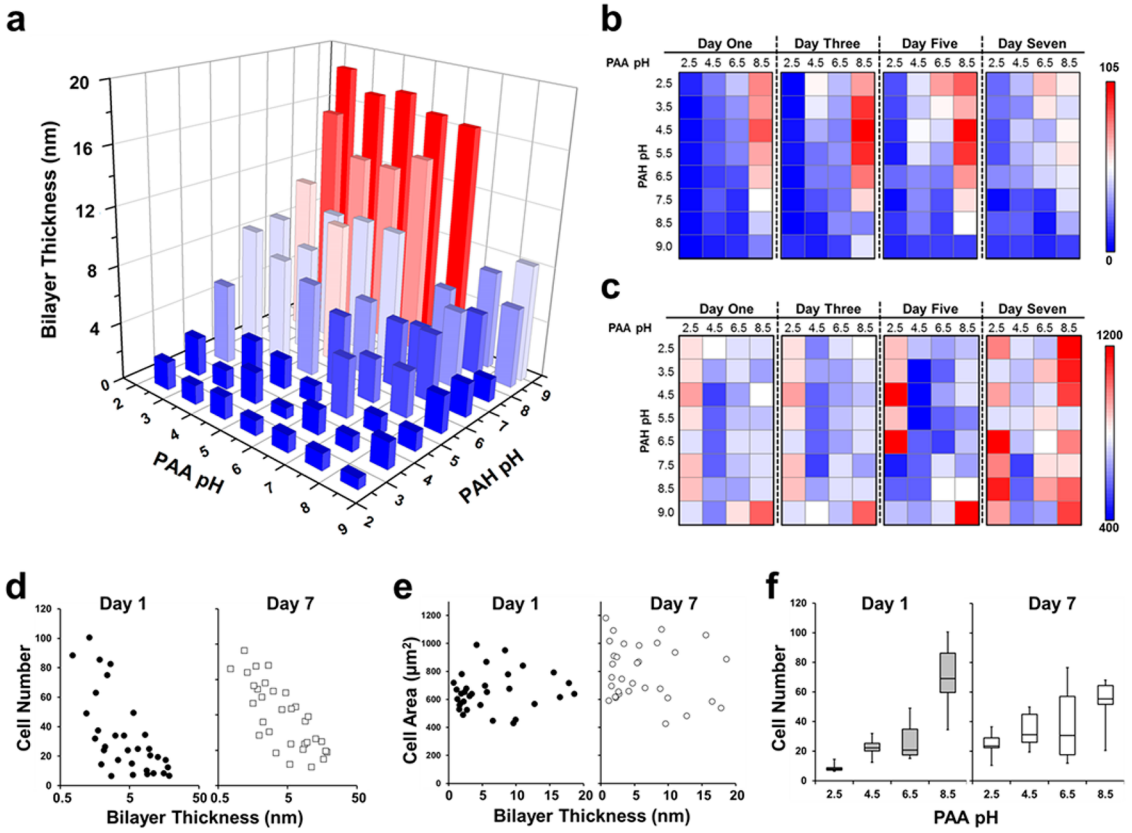

Figure 3. High-throughput screening of LbL assemblies. (a) pH-dependent thickness behavior of sequentially absorbed layers of weak polyelectrolytes, 10 bilayers. (b) NIH-3T3 cell density on films. Cells were initially seeded at 0.1 M/mL. Units = cells/mm^2. (c) Average spread area of cells on the different film architectures. Units = μm^2. (d) Effect of film thickness on cell density. Increasing bilayer thickness negatively impacted the total number of cells that initially seeded on the films. (e) Plot of cell spread area *vs* bilayer thickness. No correlation was apparent. (f) Effect of PAA pH on the cell density on the films. Higher PAA pH corresponded with increased cell density, regardless of PAH pH. Channels used were 500 μm wide and 5.0 mm long.

described by other research groups.[31−34] The microwell features contained within the CF-LbL device are recessed into the PDMS mold and as such are positioned outside of the flow of the main channel and can thus enable cell seeding on the recessed surface features. This is accomplished by first filling the channel with a cell suspension and flipping the device such that gravity directs the cells into the PDMS wells. After 30 min fresh media is flowed through the channel by pipet, and the cells not contained within the microwells are swept away. Using CF-LbL, these microwells can be coated with films that contain cell-binding moieties or have interesting cell response behaviors to examine cell viability, adhesion, mobility, proliferation, and other cellular activity. To demonstrate this application, we used a fluorescent NIH-3T3 cell line and captured cells within a microwell design (Figure 2c1). Cells were observed to preferentially seed within the microwell structures and to spread within these features after 1 day in culture (Figure 2c2).

To demonstrate the capability of CF-LbL to investigate large LbL film libraries, we performed a classic experiment first described by Rubner and co-workers,[35,36] wherein the weak polyelectrolyte bilayer film of PAA/PAH is assembled using polymer solutions that range in pH from 2.5 to 9.0 (Figure 3a). Changing the pH of a polyelectrolyte solution alters the degree of ionization of the adsorbing polymer and, as such, alters the adsorption of the polyelectrolyte to the surface. It was observed that increasing the degree of ionization of either PAA or PAH in solution led to a decreased average bilayer thickness, whereas conditions where both polyelectrolytes are weakly ionized lead to the thickest films.

These trends in pH and film thickness closely resemble those previously reported,[35,36] demonstrating the applicability of this method to traditional LbL film systems; furthermore, we were able to expand the range of pH values and conditions used in the original study.

Creating biological interfaces that modify cell behavior is an important and growing application for LbL films.[37−41] Investigating the myriad of potential iterative film assemblies around one simple film architecture however can be a very time- and material-intensive task, especially when considering the need to sterilize each sample prior to *in vitro* evaluation. In addition to preparing the samples for *in vitro* experimentation, actually conducting experiments *in situ* with large sample numbers presents many logistical

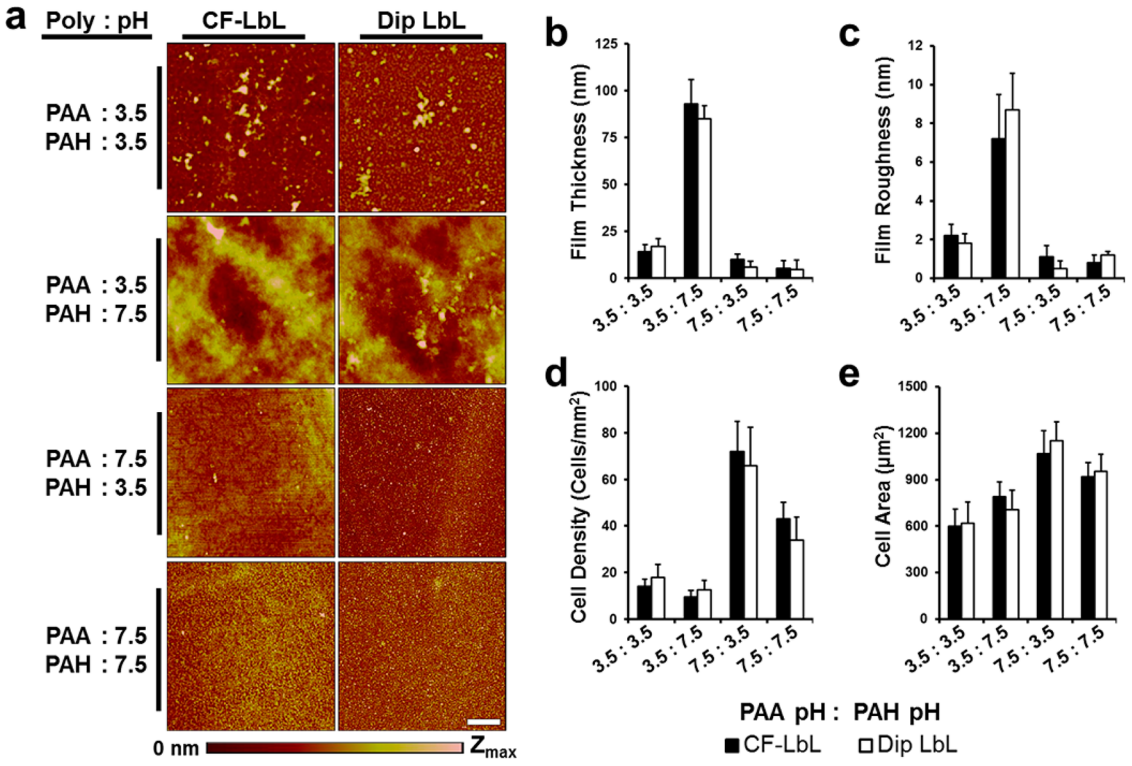

Figure 4. Comparison of $(PAA/PAH)_{10}$ films prepared via dip LbL or CF-LbL techniques. (a) AFM micrographs showing the different topograhphies for each of the LbL films assembled. (b) Film thickness of the assemblies as measured by profilometry. (c) Film roughness as measured by AFM. (d) NIH-3T3 cell density after 3 days of growth on film-coated glass. (e) Average cell spread area for a cell adhered to the film surface. Data shown as mean ± SD. Channels used were 500 μm wide and 5.0 mm long.

issues and complicates investigations significantly. A major advantage of the CF-LbL method is that the sterility of the device in which the films are assembled is easily maintained throughout the assembly process. Further, *in vitro* tests can be readily performed directly within the assembled device, greatly simplifying the setup for investigations and limiting complications from film and sample handling.

To demonstrate the application of the CF-LbL assembly in performing *in vitro* investigations, we evaluated 32 different film architectures from the previously investigated PAA/PAH bilayer system, covering a wide range of assembly conditions. NIH-3T3 cells were seeded directly onto the film and cultured for 1 week. Response to the different films was evaluated by measuring cell adherence to the surface along with proliferation. Cell density and average cell spread area were measured daily using phase contrast light microscopy (Figure 3b,c). Increasing bilayer thickness correlated significantly with decreased cell density, while no trends were apparent in regard to cell spread area (Figure 3d,e). It was also observed that the pH of PAA and PAH had a significant impact on cell density (Figure 3f).

We were interested in determining how well the CF-LbL assembled films approximated LbL films assembled via the traditional dip LbL technique. To do this, we chose four films from the previous experiment and assembled them by both dip LbL and the CF-LbL technique. We assessed both the physical characteristics of the assembled films and the cell response to them. Atomic force micrographs (AFMs) of the films assembled by either method were seen to have very similar topographies and surface roughness (Figure 4a). The average bilayer thickness and roughness of each film was measured after 10 bilayers were assembled. There was no significant difference between the films assembled by either technique (Figure 4b,c). We used NIH-3T3 cells to assess cell response. The total number of cells seeded for each group was corrected for the area upon which we were seeding. Cells were observed to respond similarly on both surfaces, with thick films leading to reduced cell density. These findings closely resemble those presented in previous reports for PAA/PAH bilayer systems, for which it was found that the mechanical stiffness of the thicker films was a primary determinant of cell adhesion.[42]

Locally delivering nucleic acids from surfaces is a relatively simple and highly adaptable approach to alter nearby gene expression, which opens significant opportunities in fields ranging from fundamental molecular biology to tissue engineering.[28,43,44] There are numerous factors that impact transfection of material, including nucleic acid packaging, material release, endosomal escape, and if necessary nuclear transport. In particular, the type of polycation used, including

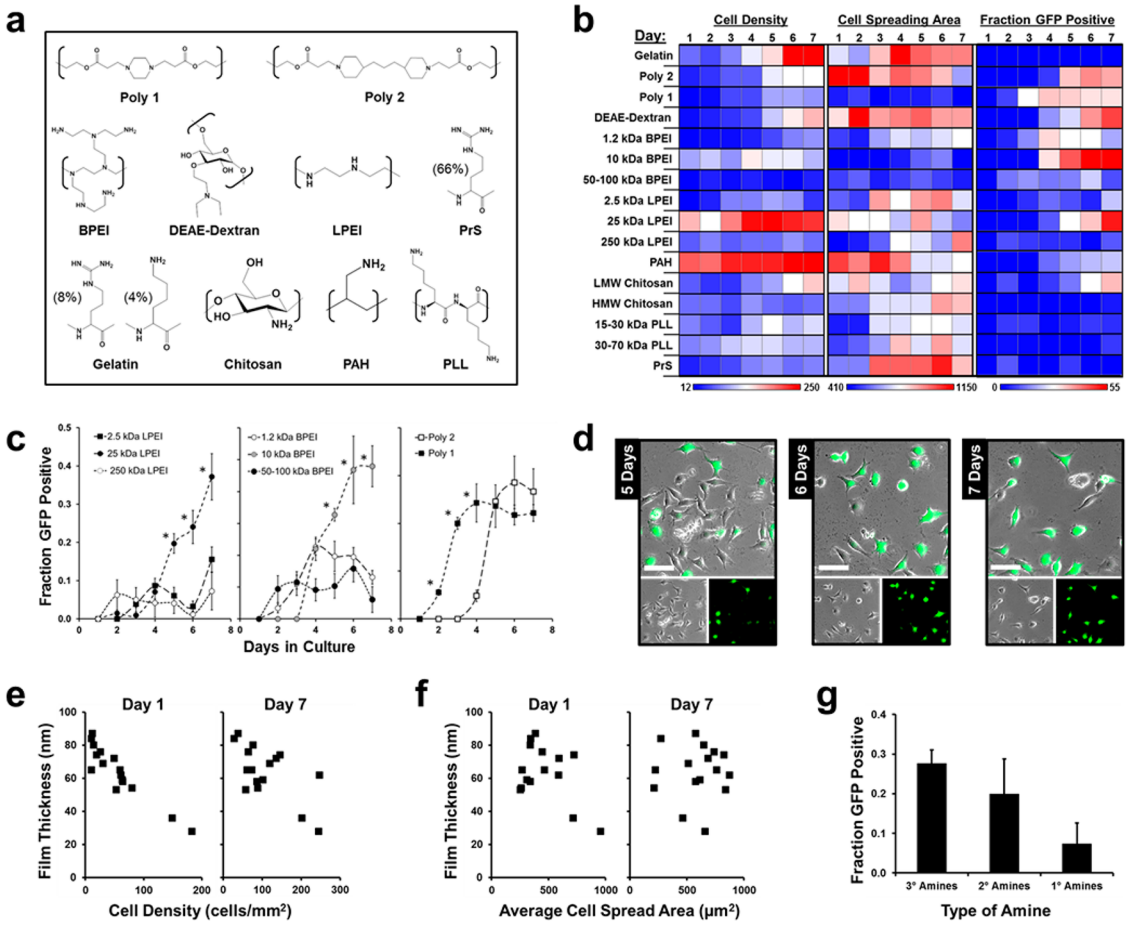

Figure 5. Polycation library screen of DNA transfection from LbL films. (a) Chemical structures of polycation repeat units. (b) Heat maps of cell density, cell spreading area, and fraction GFP of DNA transfection of cells cultured on films. (c) Transfection from films containing similar polycations of differing molecular weights. (d) Cells on $(BPEI/pEGFP)_{10}$ film cultured within the microchannels after 5, 6, and 7 days of culture. Scale bar = 50 μm. (e) Effect of film thickness on cell density at 1 and 7 days in culture. (f) Effect of film thickness on average cell spread area. (g) Effect of amine type on DNA transfection after 1 week in culture. Polycations that contained tertiary amines (3°) achieved significantly higher transfection levels than those that contained only primary amines (1°). Data shown as mean ± SD. Channels used were 1.2 mm wide and 5.0 mm long.

primary, secondary, or tertiary amines and relative hydrophobicity of the backbone, affects the loading of DNA and RNA, the nature of ionic cross-linking and complexation, and the ability of the nucleic acid to be released from the endosome and to access cells.[45,46] Due to this complexity, investigations into LbL systems for these applications face very substantial challenges.

Previously, research groups have described LbL systems capable of the local delivery of DNA from coated surfaces.[47,48] These reports provide a great deal of promise for future applications of LbL in combination with medical devices[49,50] and as DNA vaccine depots.[11,51] At this time, however, investigations can only reasonably study individual LbL systems, often assembled using only one set of assembly conditions.[47,48] To demonstrate the use of the CF-LbL assembly for screening film libraries, we decided to apply the technique to investigate a focused group of candidate films consisting of a broad range of polycations identified from literature that have been used for DNA transfection (Figure 5a). We assembled bilayer films of the polycations with a DNA plasmid for green fluorescent protein (GFP). HeLa cells were seeded directly onto the films within the device and were monitored for GFP expression, cell density, and average cell spread area every day for 7 days in culture (Figure 5b–d).

From a screen of 16 films, we found a diversity of cellular response and transfection efficacies that show some interesting trends. Cell density, measured as the number of live cells per square millimeter, was highest on the $(PAH/pEGFP)_{10}$ film, which reached near confluence after only 3 days of culture. The only two other films to reach confluence within 1 week were $(Gelatin/pEGFP)_{10}$ and $(LPEI\ 25\ kDa/pEGFP)_{10}$. Initial cell seeding density was observed to correlate inversely to film thickness, which was largely maintained after 1 week in culture (Figure 5e). Film thickness however was not observed to correlate with cell spreading, similar to what was observed for the PAA/PAH systems (Figure 5f). The primary goal of screening a diverse group of polycations was to elucidate characteristics

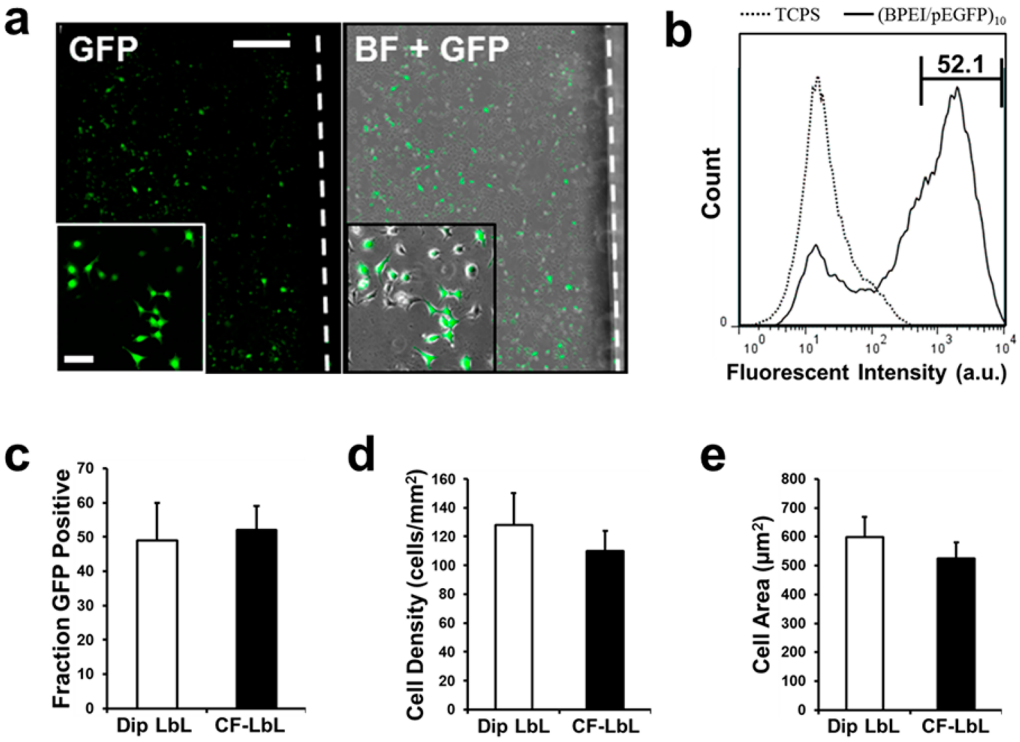

Figure 6. Large-scale reproduction of best performing architecture shows similar behavior. (a) Analysis of transfection of HeLa cells cultured on $(BPEI/pEGFP)_{10}$-coated microscope slides. BF = bright field. Scale bar = 500 μm, inset scale bar = 50 μm. (b) Flow cytometry analysis of GFP expression for HeLa cells cultured on $(BPEI/pEGFP)_{10}$ for 1 week. (c) Fraction of GFP-positive HeLa cells cultured on either dip LbL or CF-LbL coated glass after 1 week. (d) Average cell density on film-coated substrates after 1 week in culture. (e) Average cell spread area for HeLa cells seeded on films prepared by either dip LbL or CF-LbL methods. Data shown as mean ± SD.

that correlate with transfection efficacy.[52] The major trait that was seen to correlate with transfection was the type of amine, where films that consisted of polycations that contained tertiary amines achieved the highest average transfection efficacy, while those with only primary amines achieved the lowest on average (Figure 5g).

The best performing film architecture from this screen was determined to be $(BPEI/pEGFP)_{10}$, as it reached the highest fraction of GFP-expressing cells with relatively high cell density. BPEI, which presents primary, secondary, and tertiary amines, is known for its ability to both effectively complex nucleic acids and to buffer at endosomal pH, which can cause endosomal osmolytic swelling and subsequent nucleic acid release to the cytosol.[53−55] This film was evaluated on a larger scale by assembling it on microscope slides. HeLa cells were cultured on these large LbL-coated slides for 7 days (Figure 6a,b). Cell behavior and GFP expression were then analyzed. The fraction of GFP-expressing cells as well as average cell density and average cell spread area on the larger film closely resembled that of cells cultured within the CF-LbL microchannels (Figure 6c−e). Together these data provide strong support for the capability of CF-LbL to investigate LbL films for use in applications on larger scales. The films assembled by CF-LbL within microchannels performed identically to their counterparts assembled by dip LbL on a scale about a 1000 times larger in surface area.

CONCLUSIONS

In summary, we have described a method for the high-throughput assembly and screening of LbL films. We used this method for three demonstrations: (1) a study on the effect of pH on weak polyelectrolytes in LbL film assembly, (2) the *in situ* examination of cell adhesion and viability on LbL assemblies, and (3) the investigation of a library of films for DNA transfection from surfaces. This method is paired with a simple modular microfluidic device that can be used for the simultaneous assembly of hundreds of independent films or for smaller, more focused benchtop investigations. The device is fabricated *via* common soft lithography techniques and when assembled provides a sterile environment where sensitive biological analysis can be performed on each film independently.

The potential applications of LbL film assemblies are incredibly diverse and growing. Here we have provided a method using a simple microfluidic device that makes possible the high-throughput screening of LbL assemblies while significantly reducing the amount of material used. This method represents a simple yet significant advance for the investigation of LbL films while expanding the ability to study these coatings to

laboratories that previously could not. We anticipate that this approach could have enormous impact in a broad range of fields that include developing drug delivery systems and creating biological interfaces.

METHODS AND MATERIALS

Materials. Linear polyethylenimine (LPEI, M_w of 2.5K, 25K, 250K) and branched polyethylenimine (BPEI, M_w of 1.2K, 10K, 50−100K) were purchased from Polysciences; low molecular weight chitosan (LMW chitosan, M_w of 15−30K), high molecular chitosan (HMW Chitosan, M_w of 300K), gelatin (pH = 2.5), diethylaminoethyl-dextran (DEAE-Dextran), protamine sulfate (PrS), poly-L-lysine (PLL, M_w of 15−30K and 30−70K), and poly(allylamine hydrochloride) (PAH, M_w of 60K) were purchased from Sigma-Aldrich, and the degradable poly(beta-aminoesters) (designated Poly 1 and Poly 2) were synthesized using the method that was previously published.[56]

Device Fabrication. Master templates for preparing microfluidic channels were made with an SU-8 photoresist in bas-relief on silicon wafers. The microfluidic device was fabricated in polydimethylsiloxane by using a standard soft-lithography method.[57] In brief, masters with microchannels were prepared with features of SU-8 on silicon wafers with a diameter of 4 in. by a photolithography technique. The PDMS elastomer was prepared by mixing prepolymer with the curing agent (Sylgard 184, Dow Corning) at the weight ratio of 10:1, respectively. The mixture of the prepolymer and curing agent was then poured onto the master and cured in an oven at 75 °C for 4 h. After curing, the replica was carefully peeled off from the master, and holes with various diameters were made by a Harris micropunch at the designated positions. The patterned PDMS sheet and a glass slide were plasma treated for 90 s in a plasma cleaner chamber (PDC-3XG, Harrick, USA) and then brought into contact and immediately sealed. The thickness of the formed microchannel is approximately 100 μm. Micropatterned surfaces inside the microchannel were created by using multilayer soft-lithography as previously described.[58]

LbL Film Assembly. Material solutions were prepared at a 2 mg/mL concentration, and the pH was adjusted to the desired level. All solutions were sterile filtered using a 0.2 μm syringe filter prior to use. Material solutions were introduced to the inlet of a microchannel by pipet. Solutions are drawn into the microchannel *via* capillary force to fill the entire channel within 1−3 s. After channel filling the excess material within the inlet is recovered from the inlet. Material in solution is allowed to adsorb for a predetermined amount of time (*e.g.*, 5, 10, or 15 min), and then the channel is cleared either by vacuum or by pressurized air. The channel is then washed three times with a washing solution to remove material that is not well adsorbed to the channel surface. This process is then repeated with a complementary species for adsorption, and the entire process can be repeated to reach the desired number of layers of LbL film. After film assembly is complete the PDMS sheet can be removed from the substrate, leaving a microstrip of LbL film on the substrate. Dip LbL films were assembled using a Carl Zeiss HMS DS50 slide stainer. Films were built on either Si wafers or glass slides. Rinsing steps were performed using UltraPure DNase/RNase-Free water (Life Technologies) that was pH adjusted to match with the prior material adsorption step.

Multilayer Film Characterization. Film thickness was measured for films built on Si wafers using a Veeco Dektak (Plainview, NY, USA) surface profilometer. Surface roughness was measured using a Veeco Dimension 3100 atomic force microscope. Coating of microstructure-containing CF-LbL devices was performed using a ZEISS Axiovert 200 fluorescent and bright-field microscope.

Cell Culture and Transfection Studies. NIH-3T3 and HeLa cells were used in this work; both were purchased from ATCC (Manassas, VA, USA). NIH-3T3 cells were used to evaluate cell behavior on PAA/PAH LbL films. HeLa cells were used for all transfection studies. Cells were seeded within the CF-LbL assembly device following LbL film construction at an initial density of 0.1 M/mL and allowed to settle for 30 min, after which media was exchanged to remove unattached cells. All cell lines were cultured in Advanced-MEM with 5% FBS and 1% Pen-Strep and 2 mM L-glutamine. Media was exchanged daily by placing a droplet at the inlet and removing the waste at the exit of the microchannels. Bright-field and fluorescent imaging of cells was done with a ZEISS Axiovert 200. Images were analyzed using ImageJ image analysis software. Confocal imaging of cells seeded on microchannel walls was done with a Nikon A1R Ultra-Fast spectral confocal microscope, and three-dimensional projection was created using Velocity software. Flow cytometry was performed with a FACSCalibur flow cytometer.

Statistical Analysis. Data analysis was performed between groups using Student's *t*-test. These were rectified using ANOVA for comparisons between multiple groups. A value of $p < 0.05$ was used to indicate statistical significance.

Conflict of Interest: The authors declare no competing financial interest.

Supporting Information Available: S1: Photolithographic mask showing partial O_2 plasma treatment. S2: CF-LbL device arrangement is modular and customizable. S3: Automated CF-LbL assembly. S4: Manual CF-LbL assembly. S5: The effect of PAH pH on cell density. S6: Cell spread area and cell number compared to transfection efficacy. This material is available free of charge *via* the Internet at http://pubs.acs.org.

Acknowledgment. This research was supported in part by funding and core facilities provided by the U.S. Army Research Office under contract W911NF-07-D-0004 at the MIT Institute of Soldier Nanotechnology. This work was also supported by use of core facilities at the Koch Institute for Integrative Cancer Research (supported by the NCI under grant 2P30CA014051-39). We thank the Koch Institute Swanson Biotechnology Center for technical support, specifically the microscopy, flow cytometry, and histology cores. The authors wish to dedicate this paper to the memory of Officer Sean Collier, for his caring service to the MIT community and for his sacrifice.

REFERENCES AND NOTES

1. Decher, G. Fuzzy Nanoassemblies: Toward Layered Polymeric Multicomposites. *Science* **1997**, *277*, 1232–1237.
2. Quinn, J. F.; Johnston, A. P.; Such, G. K.; Zelikin, A. N.; Caruso, F. Next Generation, Sequentially Assembled Ultrathin Films: Beyond Electrostatics. *Chem. Soc. Rev.* **2007**, *36*, 707–718.
3. Lavalle, P.; Voegel, J. C.; Vautier, D.; Senger, B.; Schaaf, P.; Ball, V. Dynamic Aspects of Films Prepared by a Sequential Deposition of Species: Perspectives for Smart and Responsive Materials. *Adv. Mater.* **2011**, *23*, 1191–1221.
4. Schlenoff, J. B. Retrospective on the Future of Polyelectrolyte Multilayers. *Langmuir* **2009**, *25*, 14007–14010.
5. Hammond, P. T. Engineering Materials Layer-by-Layer: Challenges and Opportunities in Multilayer Assembly. *AIChE J.* **2011**, *57*, 2928–2940.
6. Hammond, P. T. Building Biomedical Materials Layer-by-Layer. *Mater. Today* **2012**, *15*, 196–206.
7. Sukhishvili, S. A. Responsive Polymer Films and Capsules *via* Layer-by-Layer Assembly. *Curr. Opin. Colloid. Interface Sci.* **2005**, *10*, 37–44.
8. Lee, J. A.; Krogman, K. C.; Ma, M. L.; Hill, R. M.; Hammond, P. T.; Rutledge, G. C. Highly Reactive Multilayer-Assembled TiO_2 Coating on Electrospun Polymer Nanofibers. *Adv. Mater.* **2009**, *21*, 1252–1256.
9. Shah, N. J.; Hyder, M. N.; Moskowitz, J. S.; Quadir, M. A.; Morton, S. W.; Seeherman, H. J.; Padera, R. F.; Spector, M.; Hammond, P. T. Surface-Mediated Bone Tissue Morphogenesis from Tunable Nanolayered Implant Coatings. *Sci. Transl. Med.* **2013**, *5*, 191.

10. Facca, S.; Cortez, C.; Mendoza-Palomares, C.; Messadeq, N.; Dierich, A.; Johnston, A. P. R.; Mainard, D.; Voegel, J. C.; Caruso, F.; Benkirane-Jessel, N. Active Multilayered Capsules for *in Vivo* Bone Formation. *Proc. Natl. Acad. Sci. U.S.A.* **2010**, *107*, 3406–3411.
11. DeMuth, P. C.; Min, Y.; Huang, B.; Kramer, J. A.; Miller, A. D.; Barouch, D. H.; Hammond, P. T.; Irvine, D. J. Polymer Multilayer Tattooing for Enhanced DNA Vaccination. *Nat. Mater.* **2013**, *12*, 367–376.
12. Jan, E.; Hendricks, J. L.; Husaini, V.; Richardson-Burns, S. M.; Sereno, A.; Martin, D. C.; Kotov, N. A. Layered Carbon Nanotube-Polyelectrolyte Electrodes Outperform Traditional Neural Interface Materials. *Nano Lett.* **2009**, *9*, 4012–4018.
13. Finnemore, A.; Cunha, P.; Shean, T.; Vignolini, S.; Guldin, S.; Oyen, M.; Steiner, U. Biomimetic Layer-by-Layer Assembly of Artificial Nacre. *Nat. Commun.* **2012**, *3*, 966.
14. Krogman, K. C.; Zacharia, N. S.; Schroeder, S.; Hammond, P. T. Automated Process for Improved Uniformity and Versatility of Layer-by-Layer Deposition. *Langmuir* **2007**, *23*, 3137–3141.
15. Izquierdo, A.; Ono, S. S.; Voegel, J. C.; Schaaf, P.; Decher, G. Dipping Versus Spraying: Exploring the Deposition Conditions for Speeding up Layer-by-Layer Assembly. *Langmuir* **2005**, *21*, 7558–7567.
16. Jiang, C.; Markutsya, S.; Tsukruk, V. V. Collective and Individual Plasmon Resonances in Nanoparticle Films Obtained by Spin-Assisted Layer-by-Layer Assembly. *Langmuir* **2004**, *20*, 882–890.
17. Chan, E. P.; Lee, J. H.; Chung, J. Y.; Stafford, C. M. An Automated Spin-Assisted Approach for Molecular Layer-by-Layer Assembly of Crosslinked Polymer Thin Films. *Rev. Sci. Instrum.* **2012**, *83*, 114102.
18. Cho, J.; Char, K. Effect of Layer Integrity of Spin Self-Assembled Multilayer Films on Surface Wettability. *Langmuir* **2004**, *20*, 4011–4016.
19. DeRocher, J. P.; Mao, P.; Han, J. Y.; Rubner, M. F.; Cohen, R. E. Layer-by-Layer Assembly of Polyelectrolytes in Nanofluidic Devices. *Macromolecules* **2010**, *43*, 2430–2437.
20. Kantak, C.; Beyer, S.; Yobas, L.; Bansal, T.; Trau, D. A 'Microfluidic Pinball' for on-Chip Generation of Layer-by-Layer Polyelectrolyte Microcapsules. *Lab Chip* **2011**, *11*, 1030–1035.
21. Garza, J. M.; Schaaf, P.; Muller, S.; Ball, V.; Stoltz, J. F.; Voegel, J. C.; Lavalle, P. Multicompartment Films Made of Alternate Polyelectrolyte Multilayers of Exponential and Linear Growth. *Langmuir* **2004**, *20*, 7298–7302.
22. Thompson, M. T.; Berg, M. C.; Tobias, I. S.; Lichter, J. A.; Rubner, M. F.; Van Vliet, K. J. Biochemical Functionalization of Polymeric Cell Substrata Can Alter Mechanical Compliance. *Biomacromolecules* **2006**, *7*, 1990–1995.
23. Zhu, Z.; Sukhishvili, S. A. Temperature-Induced Swelling and Small Molecule Release with Hydrogen-Bonded Multilayers of Block Copolymer Micelles. *ACS Nano* **2009**, *3*, 3595–3605.
24. Shchukin, D. G.; Kommireddy, D. S.; Zhao, Y. J.; Cui, T. H.; Sukhorukov, G. B.; Lvov, Y. M. Polyelectrolyte Micropatterning Using a Laminar-Flow Microfluidic Device. *Adv. Mater.* **2004**, *16*, 389–393.
25. DeRocher, J. P.; Mao, P.; Kim, J. Y.; Han, J.; Rubner, M. F.; Cohen, R. E. Layer-by-Layer Deposition of All-Nanoparticle Multilayers in Confined Geometries. *ACS Appl. Mater. Interfaces* **2012**, *4*, 391–396.
26. Yan, Y.; Bjonmalm, M.; Caruso, F. Assembly of Layer-by-Layer Particles and Their Interactions with Biological Systems. *Chem. Mater.* **2014**, *26*, 452–460.
27. Min, J.; Braatz, R. D.; Hammond, P. T. Tunable Staged Release of Therapeutics from Layer-by-Layer Coatings with Clay Interlayer Barrier. *Biomaterials* **2014**, *35*, 2507–2517.
28. Castleberry, S.; Wang, M.; Hammond, P. T. Nanolayered siRNA Dressing for Sustained Localized Knockdown. *ACS Nano* **2013**, *7*, 5251–5261.
29. Wood, K. C.; Chuang, H. F.; Batten, R. D.; Lynn, D. M.; Hammond, P. T. Controlling Interlayer Diffusion to Achieve Sustained, Multiagent Delivery from Layer-by-Layer Thin Films. *Proc. Natl. Acad. Sci. U.S.A.* **2006**, *103*, 10207–10212.
30. Unger, M. A.; Chou, H. P.; Thorsen, T.; Scherer, A.; Quake, S. R. Monolithic Microfabricated Valves and Pumps by Multilayer Soft Lithography. *Science* **2000**, *288*, 113–116.
31. Williams, C. M.; Mehta, G.; Peyton, S. R.; Zeiger, A. S.; Van Vliet, K. J.; Griffith, L. G. Autocrine-Controlled Formation and Function of Tissue-like Aggregates by Primary Hepatocytes in Micropatterned Hydrogel Arrays. *Tissue Eng., Part A* **2011**, *17*, 1055–68.
32. Yong, J.; Chen, F.; Yang, Q.; Zhang, D.; Bian, H.; Du, G.; Si, J.; Meng, X.; Hou, X. Controllable Adhesive Superhydrophobic Surfaces Based on PDMS Microwell Arrays. *Langmuir* **2013**, *29*, 3274–3279.
33. Chen, Q.; Wu, J.; Zhang, Y.; Lin, Z.; Lin, J. M. Targeted Isolation and Analysis of Single Tumor Cells with Aptamer-Encoded Microwell Array on Microfluidic Device. *Lab Chip* **2012**, *12*, 5180–5185.
34. Zaretsky, I.; Polonsky, M.; Shifrut, E.; Reich-Zeliger, S.; Antebi, Y.; Aidelberg, G.; Waysbort, N.; Friedman, N. Monitoring the Dynamics of Primary T Cell Activation and Differentiation Using Long Term Live Cell Imaging in Microwell Arrays. *Lab Chip* **2012**, *12*, 5007–5015.
35. Shiratori, S. S.; Rubner, M. F. PH-Dependent Thickness Behavior of Sequentially Adsorbed Layers of Weak Polyelectrolytes. *Macromolecules* **2000**, *33*, 4213–4219.
36. Yoo, D.; Shiratori, S.; Rubner, M. F. Controlling Bilayer Composition and Surface Wettability of Sequentially Adsorbed Multilayers of Weak Polyelectrolytes. *Macromolecules* **1998**, *31*, 4309–4318.
37. Aggarwal, N.; Groth, T. Multilayer Films by Blending Heparin with Semisynthetic Cellulose Sulfates: Physico-Chemical Characterization and Cell Responses. *J. Biomed. Mater. Res., Part A* **2014**, 10.1002/jbm.a.35095.
38. Gribova, V.; Gauthier-Rouviere, C.; Albiges-Rizo, C.; Auzely-Velty, R.; Picart, C. Effect of RGD Functionalization and Stiffness Modulation of Polyelectrolyte Multilayer Films on Muscle Cell Differentiation. *Acta Biomater.* **2013**, *9*, 6468–6480.
39. Wilson, J. T.; Cui, W.; Kozlovskaya, V.; Kharlampieva, E.; Pan, D.; Qu, Z.; Krishnamurthy, V. R.; Mets, J.; Kumar, V.; Wen, J.; *et al.* Cell Surface Engineering with Polyelectrolyte Multilayer Thin Films. *J. Am. Chem. Soc.* **2011**, *133*, 7054–7064.
40. Wittmer, C. R.; Phelps, J. A.; Saltzman, W. M.; Van Tassel, P. R. Fibronectin Terminated Multilayer Films: Protein Adsorption and Cell Attachment Studies. *Biomaterials* **2007**, *28*, 851–860.
41. Boura, C.; Muller, S.; Vautier, D.; Dumas, D.; Schaaf, P.; Claude Voegel, J.; Francois Stoltz, J.; Menu, P. Endothelial Cell-Interactions with Polyelectrolyte Multilayer Films. *Biomaterials* **2005**, *26*, 4568–4575.
42. Thompson, M. T.; Berg, M. C.; Tobias, I. S.; Rubner, M. F.; Van Vliet, K. J. Tuning Compliance of Nanoscale Polyelectrolyte Multilayers to Modulate Cell Adhesion. *Biomaterials* **2005**, *26*, 6836–6845.
43. Kharlampieva, E.; Kozlovskaya, V.; Sukhishvili, S. A. Layer-by-Layer Hydrogen-Bonded Polymer Films: From Fundamentals to Applications. *Adv. Mater.* **2009**, *21*, 3053–3065.
44. Tang, Z. Y.; Wang, Y.; Podsiadlo, P.; Kotov, N. A. Biomedical Applications of Layer-by-Layer Assembly: From Biomimetics to Tissue Engineering. *Adv. Mater.* **2006**, *18*, 3203–3224.
45. Nguyen, J.; Szoka, F. C. Nucleic Acid Delivery: The Missing Pieces of the Puzzle?. *Acc. Chem. Res.* **2012**, *45*, 1153–1162.
46. Tiera, M. J.; Shi, Q.; Winnik, F. M.; Fernandes, J. C. Polycation-Based Gene Therapy: Current Knowledge and New Perspectives. *Curr. Gene Ther.* **2011**, *11*, 288–306.
47. Jewell, C. M.; Lynn, D. M. Surface-Mediated Delivery of DNA: Cationic Polymers Take Charge. *Curr. Opin. Colloid Interface Sci.* **2008**, *13*, 395–402.
48. Jewell, C. M.; Zhang, J. T.; Fredin, N. J.; Lynn, D. M. Multilayered Polyelectrolyte Films Promote the Direct and Localized Delivery of DNA to Cells. *J. Controlled Release* **2005**, *106*, 214–223.
49. Saurer, E. M.; Jewell, C. M.; Roenneburg, D. A.; Bechler, S. L.; Torrealba, J. R.; Hacker, T. A.; Lynn, D. M. Polyelectrolyte

Multilayers Promote Stent-Mediated Delivery of DNA to Vascular Tissue. *Biomacromolecules* **2013**, *14*, 1696–1704.
50. Bechler, S. L.; Si, Y.; Yu, Y.; Ren, J.; Liu, B.; Lynn, D. M. Reduction of Intimal Hyperplasia in Injured Rat Arteries Promoted by Catheter Balloons Coated with Polyelectrolyte Multilayers that Contain Plasmid DNA Encoding PKC Delta. *Biomaterials* **2013**, *34*, 226–236.
51. DeMuth, P. C.; Li, A. V.; Abbink, P.; Liu, J.; Li, H.; Stanley, K. A.; Smith, K. M.; Lavine, C. L.; Seaman, M. S.; Kramer, J. A.; *et al*. Vaccine Delivery with Microneedle Skin Patches in Nonhuman Primates. *Nat. Biotechnol.* **2013**, *31*, 1082–1085.
52. Green, J. J.; Langer, R.; Anderson, D. G. A Combinatorial Polymer Library Approach Yields Insight into Nonviral Gene Delivery. *Acc. Chem. Res.* **2008**, *41*, 749–759.
53. Akinc, A.; Thomas, M.; Klibanov, A. M.; Langer, R. Exploring Polyethylenimine-Mediated DNA Transfection and the Proton Sponge Hypothesis. *J. Gene Med.* **2005**, *7*, 657–663.
54. Whitehead, K. A.; Langer, R.; Anderson, D. G. Knocking down Barriers: Advances in siRNA Delivery. *Nat. Rev. Drug Discovery* **2009**, *8*, 129–138.
55. Gavrilov, K.; Saltzman, W. M. Therapeutic siRNA: Principles, Challenges, and Strategies. *Yale J. Biol. Med.* **2012**, *85*, 187–200.
56. Lynn, D. M.; Langer, R. Degradable poly(beta-amino esters): Synthesis, Characterization, and Self-Assembly with Plasmid DNA. *J. Am. Chem. Soc.* **2000**, *122*, 10761–10768.
57. Xia, Y. N.; Whitesides, G. M. Soft Lithography. *Annu. Rev. Mater. Sci.* **1998**, *28*, 153–184.
58. Mata, A.; Fleischman, A. J.; Roy, S. Fabrication of Multi-layer SU-8 Microstructures. *J. Micromech. Microeng.* **2006**, *16*, 276–284.